J Mater Sci (2009) 44:1363–1373
DOI 10.1007/s10853-008-3004-4

# Sol–gel synthesis of vanadium pentoxide nanoparticles in air- and water-stable ionic liquids

**Mohammad Al Zoubi · Hala K. Farag · Frank Endres**

Received: 20 July 2008 / Accepted: 12 September 2008 / Published online: 8 October 2008


**Abstract** Vanadium pentoxide ($V_2O_5$) nanoparticles were synthesized at moderate reaction temperatures by hydrolysis of $VO[OCH(CH_3)_2]_3$ in two different air- and water-stable ionic liquids with the same anion: 1-butyl-1-methyl pyrrolidinium bis(trifluoromethylsulfonyl)amide ($[Py_{1,4}]Tf_2N$) and 1-ethyl-3-methylimidazolium bis(trifluoromethylsulfonyl)amide ($[EMIM]Tf_2N$) via the sol–gel method using acetone and isopropanol either as refluxing solvents or as co-solvents. The cation type of the ionic liquid affects the crystallinity, morphology, and surface area of the produced nanoparticles: $[Py_{1,4}]Tf_2N$ gave products with higher crystallinity especially with acetone as a refluxing and co-solvent, while $[EMIM]Tf_2N$ gave a clear mesoporous morphology with isopropanol as a refluxing solvent. Ionic liquids affect the key factors (morphology and surface area) that make $V_2O_5$ an attractive material as catalyst and/or cathodic material for lithium ion batteries.

## Introduction

Transition metal oxides are of great interest because of their fascinating optical, electrical, and magnetic properties in addition to their thermal and chemical stability. These properties can be tailored for a wide variety of applications [1].

M. A. Zoubi · H. K. Farag · F. Endres (✉)
Institute of Particle Technology, Clausthal University of Technology, 38678 Clausthal-Zellerfeld, Germany
e-mail: frank.endres@tu-clausthal.de

H. K. Farag
Inorganic Chemistry Department, National Research Centre, Dokki, Cairo, Egypt

Vanadium pentoxide ($V_2O_5$), which is a semiconductor with an optical band gap energy of 2.38 eV at room temperature, is an important transition metal oxide. This class of materials exhibits a wide range of electronic and ionic properties [2, 3].

The electronic conductivity of $V_2O_5$ arises from an electron hopping process between vanadium ions in different valance states, namely V(IV) and V(V) and occurs only in dry gels. Ionic conductivity is observed in wet gels due to surface V–OH groups and mobile protons in the water-swollen space between the layers of $V_2O_5 \cdot nH_2O$ [1, 4].

Vanadium pentoxide, which crystallizes in a layered structure, has been used for a variety of applications [5–7] such as electrochromic and optical switching devices [8, 9] and as an electrode material for electrochemical capacitors (EC) because of its low cost and its variable oxidation states [10].

A xerogel form of vanadium pentoxide is represented by $V_2O_5 \cdot nH_2O$ with water in the interlayer space, which is very weakly bound to the oxide network by hydrogen bonds [2]. The amount of intercalated water determines the distance between two layers. Vanadium pentoxide xerogel with a high interlayer distance is suited to the intercalation of a variety of guest specimen like $Li^+$ ions, which can be used as a reversible cathode material for lithium ion batteries [11–13].

Vanadium pentoxide powders can be obtained by different physical and chemical methods. For example, micro- and nano-sized powders of pure $V_2O_5$ were synthesized by decomposition of gas-phase vanadium oxytrichloride ($VOCl_3$) in oxygen/argon/hydrogen microwave plasma generated at atmospheric pressure [14]. They have also been prepared by wet processes like electrodeposition and sol–gel methods [15, 16].

The sol–gel process is an attractive method for the synthesis of metal oxides as the size and morphology of the metal oxide particles in the sol or gel during the early stages can be controlled thus leading to products with high purity and high homogeneity [17].

In this method different factors, such as the nature of alkyl groups of the metal alkoxide precursors, water/alkoxide ratio, catalyst, reaction temperature, and solvent nature affect the kinetics of the hydrolysis reaction and the structure of the obtained material. Metal alkoxides are convenient starting materials for sol–gel reactions as many of them are commercially available in high purity [18]. Moreover, metal alkoxides are rapidly hydrolyzed which gives rise to a polymerization reaction leading to the corresponding metal oxides or hydrated oxides [19].

Polarity, dipole moment and acidity of the solvent strongly affect the reaction pathway as well as the physicochemical properties of the final gel [20]. Polar protic solvents such as isopropanol are favorable as both cations and anions are stabilized by complexation via donor atoms and hydrogen bonding, respectively. Polar aprotic solvents such as acetone can, however, only solvate positively charged species [21]. Solvents can also react with metal alkoxides and change the precursor at a molecular level [22]. For this purpose, we have focused in our study on the effect of the type of organic solvent used either as a refluxing solvent or a co-solvent.

Room temperature ionic liquids (RTILs) have become quite popular as a new type of solvent in the recent few years [23]. They have been described as excellent media for organic and inorganic synthesis [24, 25]. Ionic liquids can also be used as templating agents in the synthesis of mesoporous and microporous materials and as solvents for sol–gel preparation [26–29]. RTILs are salts that are liquid at room temperature, mostly with poorly coordinated anions and cations. They are usually composed of a bulky often asymmetric organic cation and organic or inorganic anions. Ionic liquids are due to their variety good solvents for both organic and inorganic materials and most of them have negligible vapor pressures at room temperature and a good thermal stability up to, in part, 300 °C. An interesting aspect is that air- and water-stable ionic liquids can be recycled and used repeatedly, thus making synthetic processes less expensive, more efficient and environmentally friendly [30–33]. They are also considered as good solvents for the sol–gel preparation of metal oxides. The use of ILs in the sol–gel synthesis of $TiO_2$, as an example, showed quite an interesting effect on the obtained metal oxide: The ionic liquid 1-butyl-3-methylimidazolium hexafluorophosphate, [BMIM]$PF_6$ enhances the generation of very small nanocrystalline anatase particles and inhibits the aggregation of these particles [34]. The air- and water-stable ionic liquid 1-ethyl-3-methylimidazolium bis(trifluoromethylsulfonyl)amide ([EMIM]$Tf_2N$) and others have been used in the direct low temperature synthesis of rutile nanostructures [35]. The results showed interestingly that the hydrophobic anion ($Tf_2N^-$) of the IL favors rutile formation. Furthermore, the sol–gel synthesis of nanocrystalline rutile and anatase $TiO_2$ showed also quite interesting effect of the cation-type of the ionic liquid on the phase type and morphology of the produced nanoparticles [36].

In the present paper, we report on the synthesis and characterization of vanadium pentoxide powders in air- and water-stable ionic liquids (with the same anion), namely: [$Py_{1,4}$]$Tf_2N$ and [EMIM]$Tf_2N$ by the sol–gel method. The effect of the type of organic solvents (acetone and isopropanol) used as refluxing solvent or as a co-solvent on the metal oxide properties is also studied.

## Experimental

### Materials

The chemicals are vanadium (V) triisopropoxide oxide (95–99% $VO[OCH(CH_3)_2]_3$, Alfa Aesar), bi-distilled water, 1-butyl-1-methyl pyrrolidinium bis(trifluoromethylsulfonyl)amide ([$Py_{1,4}$]$Tf_2N$ ultra pure, Merck), 1-ethyl-3-methylimidazolium bis(trifluoromethylsulfonyl)amide, ([EMIM]$Tf_2N$, ultra pure Merck), isopropanol (assay (GC) min 99.9% *i*-PrOH, $(CH_3)_2CHOH$, Sigma-Aldrich), and acetone (99.5% anhydrous, $CH_3COCH_3$, Alfa Aesar). All chemicals are used without further purification. All handling of the ionic liquids and of the vanadium precursor was done in an argon-filled glove box with $H_2O$ and $O_2$ <1 ppm.

### Synthesis of vanadium pentoxide nanocrystallites

Vanadium pentoxide has been prepared in two different solvents: in pure ionic liquids and in mixtures of ionic liquids and organic solvents (isopropanol and acetone separately). The following procedures are performed after optimization of some reaction parameters like: precursor-to-ionic liquid volume ratio, water-to-precursor volume ratio, and the hydrolysis temperature.

#### *Synthesis in ionic liquids*

Five milliliters of $VO[OCH(CH_3)_2]_3$ were added to 20 mL of the ionic liquids [$Py_{1,4}$]$Tf_2N$ and [EMIM]$Tf_2N$ in an argon-filled glove box. The mixtures were then transferred in closed vessels out of the glove box and stirred for about 1 h at 70 °C to get homogenous mixtures. The hydrolysis was performed by dropwise adding of 2.5 mL of bi-distilled water at 70 °C. Red-orange viscous $V_2O_5$ gels were

obtained instantaneously upon the addition of water into the $VO[OCH(CH_3)_2]_3$/IL mixture. After 1 h of continuous stirring, the reaction flasks were moved to an ultrasonic bath for another 1 h in order to release trapped water. To enhance the gelation process, the temperature was then raised to 100 °C under ongoing stirring and left for 24 h. The mixture became a black-green colored gel. Ionic liquids as well as organic residues were removed from the gel network by refluxing the gels at 75 °C for about 24 h in isopropanol. After that the gel was separated by centrifugation and soaked in isopropanol overnight. Then, it was washed with isopropanol and acetone several times and finally dried at room temperature under vacuum overnight to get it as powder. In the case of using acetone instead of isopropanol as a refluxing solvent at 53 °C, denser $V_2O_5 \cdot nH_2O$ gels were obtained which convert to xerogels after 7 days of aging at room temperature. Longer aging times in partially closed beakers lead to condensed disks. To get the product as powder, the disk was crumbed ultrasonically and washed several times by acetone and isopropanol. The isothermal annealing of the powder was performed under air with a heating rate of 10 °C/min and held at the desired temperature value for 1 h.

*Synthesis in mixtures of ionic liquid with isopropanol or acetone*

Five milliliters of $VO[OCH(CH_3)_2]_3$ were added to 10 mL of the ionic liquid ($[Py_{1,4}]Tf_2N$ or $[EMIM]Tf_2N$) in the glove box. The closed vessels were then transferred outside the glove box and 10 mL of *i*-PrOH (or 10 mL acetone) were then added slowly to the mixture and stirred at 70 °C for about 1 h until a clear solution was obtained. Then, 2.5 mL of bi-distilled water were added dropwise with continuous stirring. After 1 h, the reaction flask was moved to an ultrasonic bath for another 1 h to release trapped water. The reaction flask was connected to a condenser so that gelation and refluxing processes occur at the same time. The temperature was then raised to 100 °C for 24 h.

The procedure for $V_2O_5$ synthesis in the different solvents is given in Scheme 1, and the abbreviations of all samples are given in Table 1.

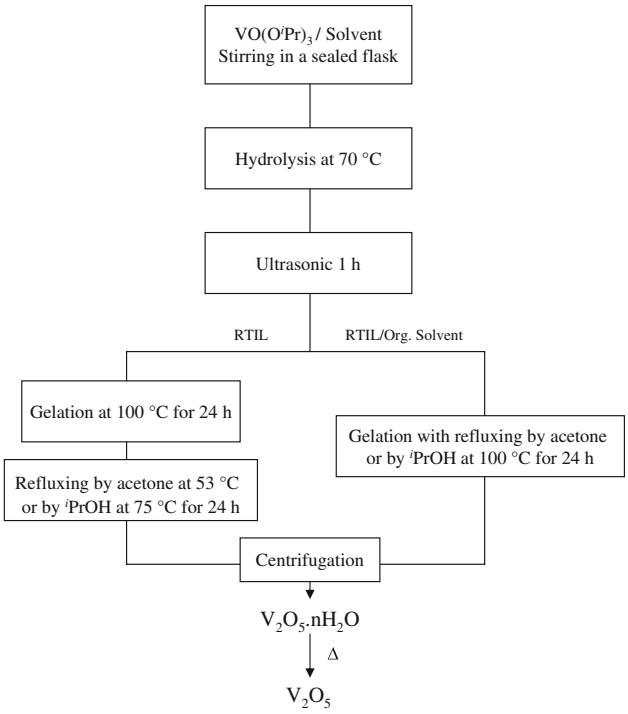


**Scheme 1** The procedure of preparation of $V_2O_5$ powders

## Characterization

The crystallinity of the vanadium pentoxide powders was checked by powder X-ray diffraction (XRD) with a Siemens D-500 diffractometer using Co$K\alpha$ (1.78897 Å) radiation at 41 kV and 40 mA. The Scherrer formula was applied using the (001) peak to determine the particle size, ($D = 0.89\ \lambda/\beta\cos\ \theta$; where $D$ is the crystallite size (nm); $\lambda$, the wavelength of the radiation Co$K\alpha$ (nm); $\beta$, the angular width of the peak at half maximum height (radians); and $\theta$, characteristic diffraction angle (radians). All of the XRD measurements were performed on the samples without annealing unless otherwise stated. Calcined samples were heated in the presence of air with a heating rate of 10 °C/min to the desired temperature for 1 h. The surface morphology of the products was investigated by using a high-resolution field emission scanning electron microscope (HR-SEM, Carl Zeiss DSM 982 Gemini). Thermal gravimetric analysis (TGA) and differential thermal analysis (DTA) were carried out on a NETZSCH STA 409 PC thermal analyzer at a heating rate of 10 °C/min starting from room temperature to 800 °C in air. The surface area of the powders was determined by Brunauer–Emmett–Teller (BET) measurements.

All of the mentioned measurements were performed on samples prepared by water hydrolysis of $VO[OCH(CH_3)_2]_3$ unless otherwise mentioned.

## Results and discussion

### $V_2O_5$ from the pure ionic liquids

Vanadium pentoxide is prepared in two different ionic liquids: $[Py_{1,4}]Tf_2N$ and $[EMIM]Tf_2N$ (Scheme 2) with different organic solvents (acetone and isopropanol) as refluxing solvents. Figure 1 shows a comparison between the XRD patterns of vanadium pentoxide powders prepared in the two ionic liquids using acetone and isopropanol

**Table 1** The abbreviations of $V_2O_5$ samples prepared in different solvent media

| Sample abbreviation | Solvent media | Sample abbreviation | Solvent media |
|---|---|---|---|
| $P_r$a | [**Py**$_{1,4}$]$Tf_2N$ **r**efluxing by **a**ceton | $I_r$a | [EM**I**M]$Tf_2N$ **r**efluxing by **a**ceton |
| $P_r$i | [**Py**$_{1,4}$]$Tf_2N$ **r**efluxing by isopropanol | $I_r$i | [EM**I**M]$Tf_2N$ **r**efluxing by **i**sopropanol |
| $P_c$a | [**Py**$_{1,4}$]$Tf_2N$ **c**o-solvent with **a**cetone | $I_c$a | [EM**I**M]$Tf_2N$ **c**o-solvent with **a**cetone |
| $P_c$i | [**Py**$_{1,4}$]$Tf_2N$ **c**o-solvent with **i**sopropanol | $I_c$i | [EM**I**M]$Tf_2N$ **c**o-solvent with **i**sopropanol |

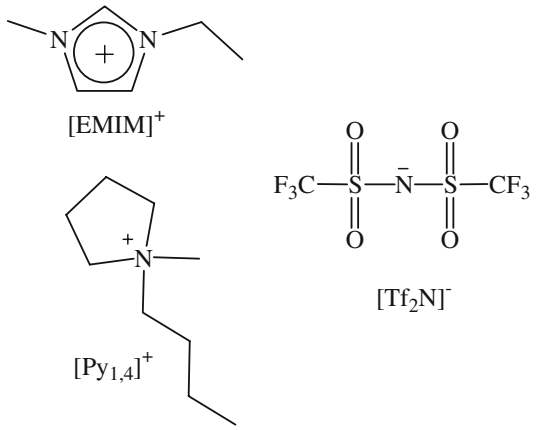


**Scheme 2** Structures of ionic liquids

separately as refluxing solvents. In the case of acetone, [Py$_{1,4}$]$Tf_2N$ gives powders with higher crystallinity whereas no significant difference between the two ionic liquids was observed when isopropanol was used. This might be attributed to the different interaction of the organic cations $[Py_{1,4}]^+$ and $[EMIM]^+$ with the surface oxygen atoms of $V_2O_5 \cdot nH_2O$ which gives rise to a more ordered structure. The solvent can affect these interactions since isopropanol interacts more strongly with the surface oxygens (V=O) than the organic cations via hydrogen bonding. Moreover, both [Py$_{1,4}$]$Tf_2N$ and [EMIM]$Tf_2N$ are more soluble in isopropanol than in acetone which slightly eliminates the effect of the ionic liquids on the crystallinity of the product (Fig. 1b). Acetone is an aprotic solvent, thus the organic cation interacts better with the surface oxygen atoms of $V_2O_5$. This interaction is more significant when $[Py_{1,4}]^+$ is employed because the positive charge in $[EMIM]^+$ is delocalized in the aromatic imidazolium ring. The best XRD pattern was obtained for the hydrated $V_2O_5$ disk, prepared in [Py$_{1,4}$]$Tf_2N$ (sample $P_r$a) with acetone as a refluxing solvent as shown in Fig. 2.

The type of the ionic liquid as well as the refluxing solvent also affects the morphology of the obtained $V_2O_5$ powders. Figure 3 shows high resolution scanning electron micrographs (HR-SEM) of the samples prepared in the two ionic liquids. The powders obtained from [EMIM]$Tf_2N$ are more porous and show rather a mesoporous morphology. Such a morphology was also reported for the rutile phase of $TiO_2$ [28], which was prepared in [BMIM]$BF_4$ ionic liquid by the sol–gel method, and it was explained that the special molecular structure and property of such imidazolium-based ionic liquids (a hydrogen bond-*co*-$\pi$-$\pi$ stack mechanism) is responsible for the formation of the mesoporous structure. The morphology difference is more significant when refluxing the gels with isopropanol as the powders are more porous (Fig. 3b and d). This can be ascribed to

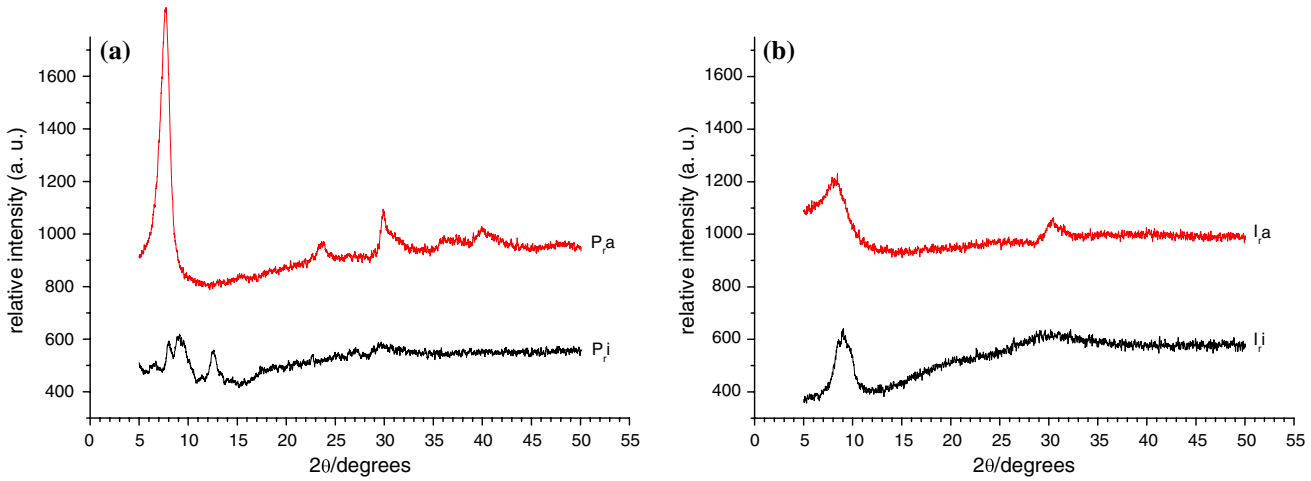


**Fig. 1** XRD patterns of as-prepared $V_2O_5$ powder samples prepared in two different ionic liquids: **a** [Py$_{1,4}$]$Tf_2N$, **b** [EMIM]$Tf_2N$. See Scheme 2

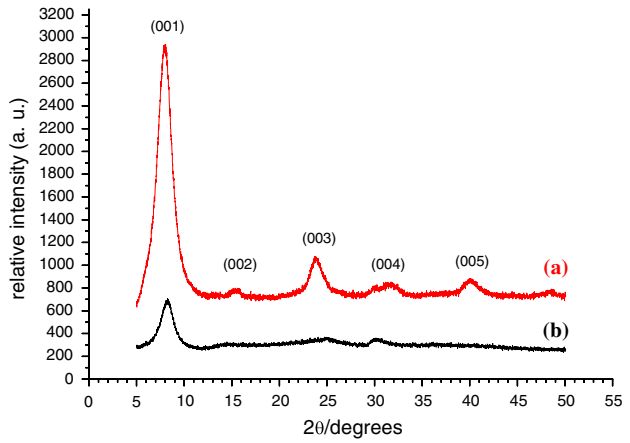


**Fig. 2** XRD patterns of as-prepared $V_2O_5$ disks in: (a) $[Py_{1,4}]Tf_2N$ and (b) $[EMIM]Tf_2N$

higher solubility of the employed ionic liquids in isopropanol than in acetone, giving rise to formation of porous powders. This suggests that the employed ionic liquids act as templates. In further experiments, hydrochloric acid (25% assays) was used instead of water to hydrolyze the same vanadium precursor in both ionic liquids and under the same conditions with acetone as a refluxing solvent. Acid catalysis promotes the protonation of isopropoxy groups. Thus, the vanadium atoms become more electrophilic and consequently more susceptible to water attack. Figure 4 shows HR-SEM images of $V_2O_5$ obtained in $[Py_{1,4}]Tf_2N$ and $[EMIM]Tf_2N$ by acidic hydrolysis. A rod-like structure is obviously seen especially with the sample prepared in $[Py_{1,4}]Tf_2N$ (Fig. 4a). The surface area of this sample was strongly enhanced (58 $m^2/g$ compared with

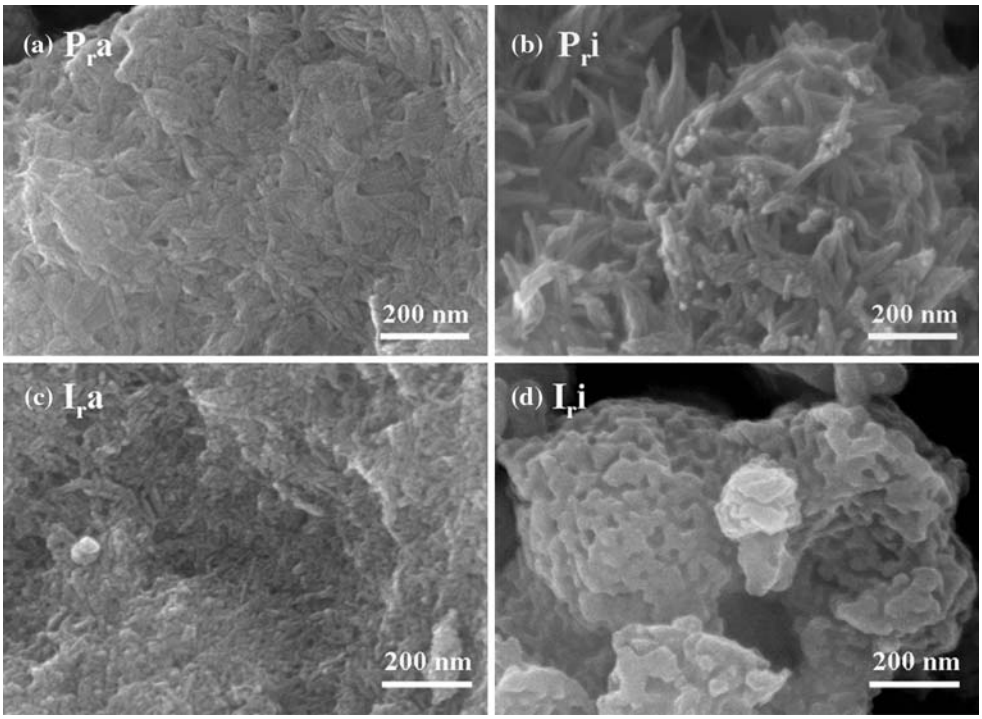


**Fig. 3** HR-SEM micrographs of $V_2O_5$ powder samples: **a** $P_r$a, **b** $P_r$i, **c** $I_r$a and **d** $I_r$i. See Table 1 for abbreviations

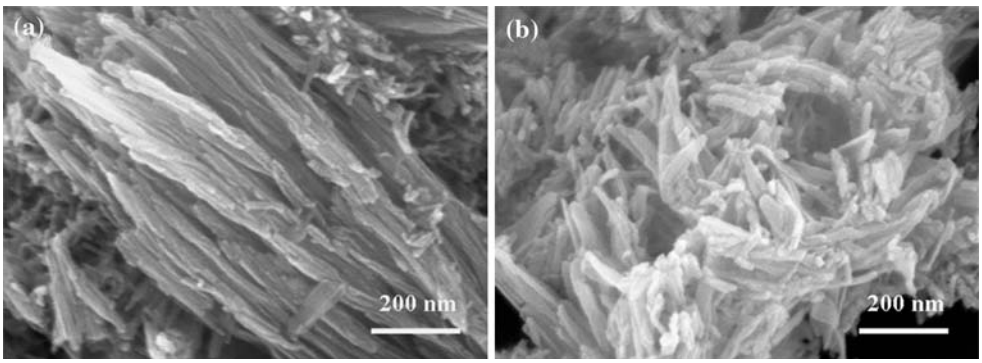


**Fig. 4** HR-SEM micrographs of $V_2O_5$ powder samples prepared by acid hydrolysis in: **a** $[Py_{1,4}]Tf_2N$ and **b** $[EMIM]Tf_2N$

<3 $m^2/g$ for the corresponding synthesis by water hydrolysis) and [EMIM]$Tf_2N$ gave 88 $m^2/g$ compared with 23 $m^2/g$ from water hydrolysis.

The XRD pattern of the prepared vanadium pentoxide (Fig. 2) shows a preferred orientation of the layered structure of $V_2O_5 \cdot nH_2O$ and is consistent with literature data [37]. This is also comparable with XRD patterns of $V_2O_5 \cdot 1.8H_2O$ xerogel prepared by acidification of an aqueous solution of sodium metavanadate ($NaVO_3$) reported by Durupthy et al. [38]. The base peak (001) of $I_r$a sample appears at a higher $2\theta$ than that of $P_r$a. This means that the amount of adsorbed water between layers in $P_r$a sample is smaller than that in $I_r$a. Barbosa et al. [39] pointed out that a shift of the (001) diffraction line to higher $2\theta$ value indicates a decrease of the interlayer spacing and thus decreasing amount of intercalated water. The calculated average particle size is around 4.7 nm for $P_r$a sample and 6.7 nm for $I_r$a. The intercalated water between $V_2O_5$ layers can be removed upon heating the xerogel to 250 °C (Eq. 1). Amorphous $V_2O_5$ is obtained at temperatures above 250 °C and orthorhombic crystals of $V_2O_5$ are formed at ~350 °C [2]:

$$V_2O_5 \cdot 1.8H_2O\ (120^\circ\ C) \rightarrow V_2O_5 \cdot 0.5H_2O\ (250^\circ\ C) \rightarrow V_2O_5 \quad (1)$$

Figure 5 shows XRD patterns of $P_r$a sample with and without annealing at various temperatures. The XRD patterns of $P_r$a sample annealed at 360, 420, and 600 °C (Fig. 5) show almost the same patterns with the same peak intensities although they have different colors as shown in Fig. 6: green-brownish at 360 °C due to the presence of residual organic materials, almost orange at 420 °C and completely bright yellow-orange at 600 °C which is the color of pure $V_2O_5$. At temperatures higher than the melting point of $V_2O_5$ (690 °C) namely, at 800 °C and 1000 °C, the color becomes orange-brown as shown in Fig. 6. The XRD patterns of both samples are the same with a very high intensity of the (001) peak relative to other peaks in the same pattern which means that the layers of the square pyramidal $V_2O_5$ units are ordered in the [001] direction [40, 41]. Losurdo et al. reported in their work on $V_2O_5$ film-deposition at various temperatures, that the appearance of the (001) reflection with higher intensity indicates that a higher degree of crystallinity with a preferential orientation and a highly ordered structure of $V_2O_5$ is obtained [42]. The XRD patterns of all annealed samples (Fig. 5) are consistent with the data available in the JCPDS file No. 41-1426 diffraction file for orthorhombic $V_2O_5$.

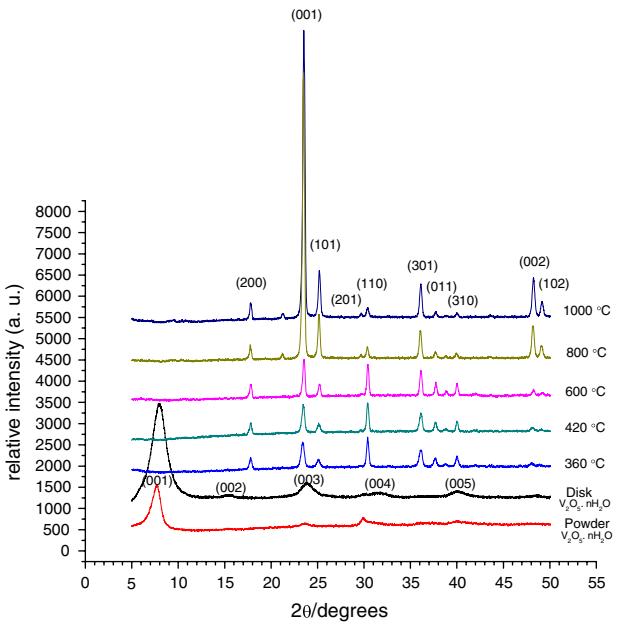


**Fig. 5** XRD patterns of $P_r$a samples: as-prepared disk, powder, and calcined powders at various temperatures

The SEM images of $V_2O_5$ powders annealed at various temperatures are shown in Fig. 7. At 420 °C, the powder contains fine crystallites with several hundreds nanometer in diameter (Fig. 7a). Interestingly, the SEM image of the sample annealed at 600 °C (Fig. 7b and c) shows microcrystals (orthorhombic prisms) of $V_2O_5$ with terraces. The SEM images of the sample annealed at 800 °C, a temperature above the melting point of $V_2O_5$, show a layered structure (Fig. 7d).

Differential thermal analysis is performed on the samples in order to give more information on the crystallization temperature and the melting points. Figure 8 shows the DTA curves of all samples. There are two exothermic peaks for almost all of the samples located at around 360 and 420 °C: the first peak can be assigned to the combustion of residual ionic liquid and other organic impurities. The second peak might be attributed to the oxidation of some present vanadium (IV) to vanadium (V). The endothermic sharp peak at 680 °C refers to the melting point of $V_2O_5$.

Thermogravimetry (TGA) was used to determine the percentage of $V_2O_5$ in the prepared samples. Figure 9 shows thermograms of vanadium pentoxide samples prepared in the two ionic liquids with refluxing by isopropanol and acetone separately. As shown in Fig. 9, all thermograms show the same general features. A small weight loss in the temperature range of 30–300 °C is observed due to the dehydration of $V_2O_5 \cdot nH_2O$. Then a sharp decrease in the weight is recorded up to a temperature of about 400 °C as a result of the combustion of residual ionic liquid and other organic impurities. All of the samples showed weight increase by about 1.5–2.0% at temperatures between 380 and 450 °C. This might be attributed to the oxidation of $VO_2$, formed due to the incomplete hydrolysis [43], to


**Fig. 6** Photographs of $P_r$a samples: as-prepared disk, powder, and calcined powders at various temperatures

$V_2O_5$. The presence of $V^{4+}$ results also in green coloration of the sample [44]. Livage et al. pointed out that the formation of the reduced oxide $VO_2$ appears to be much easier when alkoxides are used as precursors rather than aqueous vanadates because of the reducing power of the non-hydrolyzed alkoxy groups [45]. The presence of $VO_2$ species led to further oxidation to $V_2O_5$ upon continuous heating, thus a weight gain of 1.5–2.0% occurs [46]. The presence of $V^{4+}$ enhances the electrical conductivity of $V_2O_5$, since electronic conductivity occurs through the electron-hopping process between $V^{4+}$ and $V^{5+}$ ions [1, 4].

The extent of weight loss of the samples obtained using isopropanol as a refluxing solvent is higher than those of samples obtained using acetone. Furthermore, the major weight loss in samples $P_r$i and $I_r$i is observed at higher temperatures (at about 400 °C) compared with samples $P_r$a and $I_r$a (at about 300 °C, Fig. 9). This might be attributable to bounding of some isopropoxy groups to surface vanadium atoms. It was reported that alkoxy ligands bounded to the oxide network are only removed upon heating above 300 °C [45]. Therefore, the recorded weight loss is higher in case of using isopropanol as a refluxing solvent.

It is worth noting that $V_2O_5$ can react with isopropanol producing vanadyl triisopropoxide $VO(O^iPr)_3$ in a reversible reaction [46] according to (Eq. 2):

$$V_2O_5 + 6(CH_3)_2CHOH \rightleftarrows 2VO\left[OCH(CH_3)_2\right]_3 + 3H_2O \quad (2)$$

We have found that re-hydrolysis of the clear filtrate obtained after refluxing of the gel with isopropanol gives hydrated vanadium oxide. This indicates the presence of $VO(O^iPr)_3$ after refluxing with isopropanol.

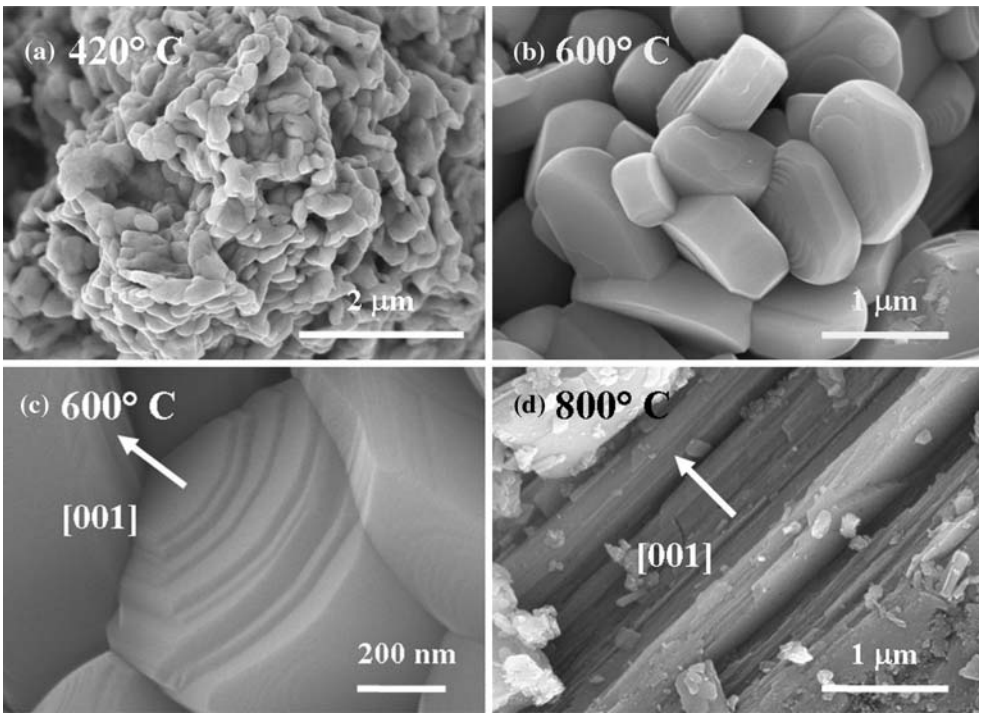


**Fig. 7** HR-SEM micrographs of calcined powders of $P_r$a sample at various temperatures: **a** 420 °C, **b** 600 °C, and **c** 800 °C

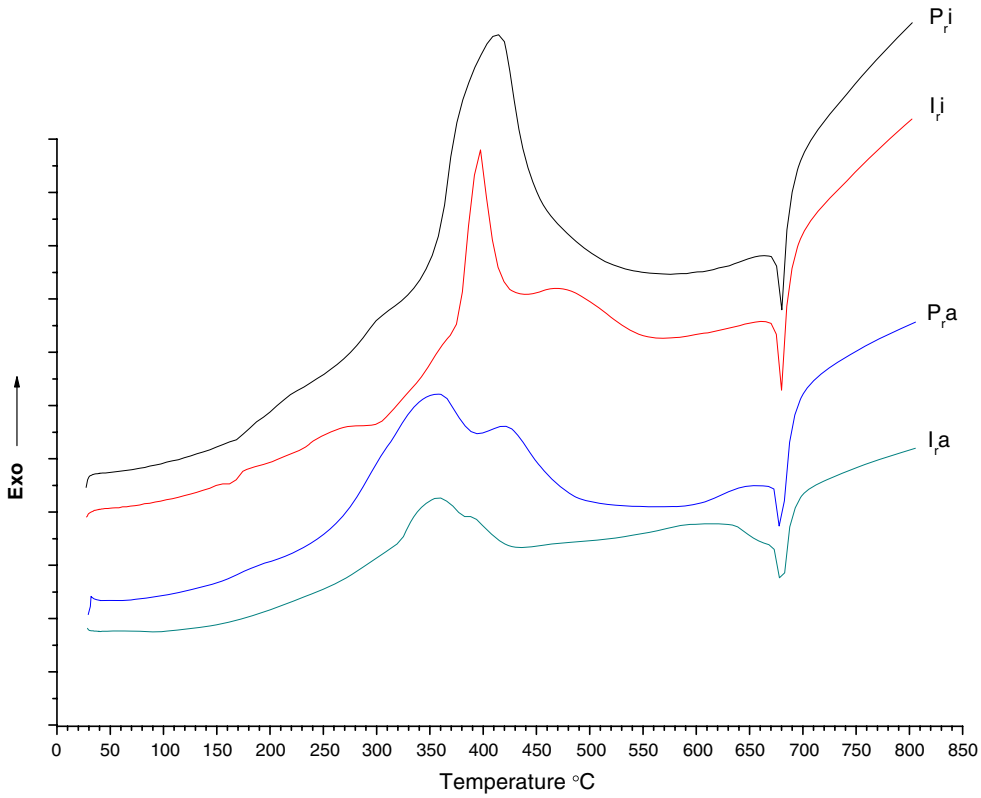


**Fig. 8** DTA curves of $V_2O_5 \cdot nH_2O$ powder samples prepared from the two ionic liquids with acetone and isopropanol (separately) as refluxing solvents. See Table 1 for abbreviations

$V_2O_5$ from ionic liquid/organic solvent mixtures

From our results on the sol–gel synthesis of $TiO_2$, mixing an organic solvent (acetone or isopropanol) with ionic liquids as media for the hydrolysis process was feasible as in this case gelation and refluxing processes occur at the same time. Moreover, this process showed an effect on phase formation of $TiO_2$ and the morphology of the

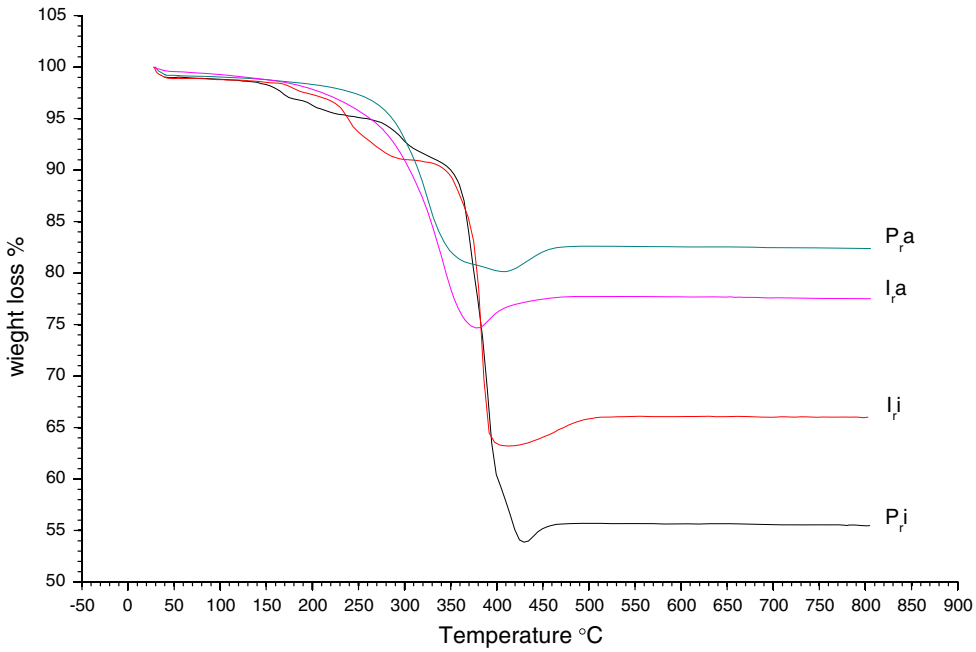


**Fig. 9** TGA curves of $V_2O_5 \cdot nH_2O$ powder samples prepared from the two ionic liquids with acetone and isopropanol (separately) as refluxing solvents. See Table 1 for abbreviations

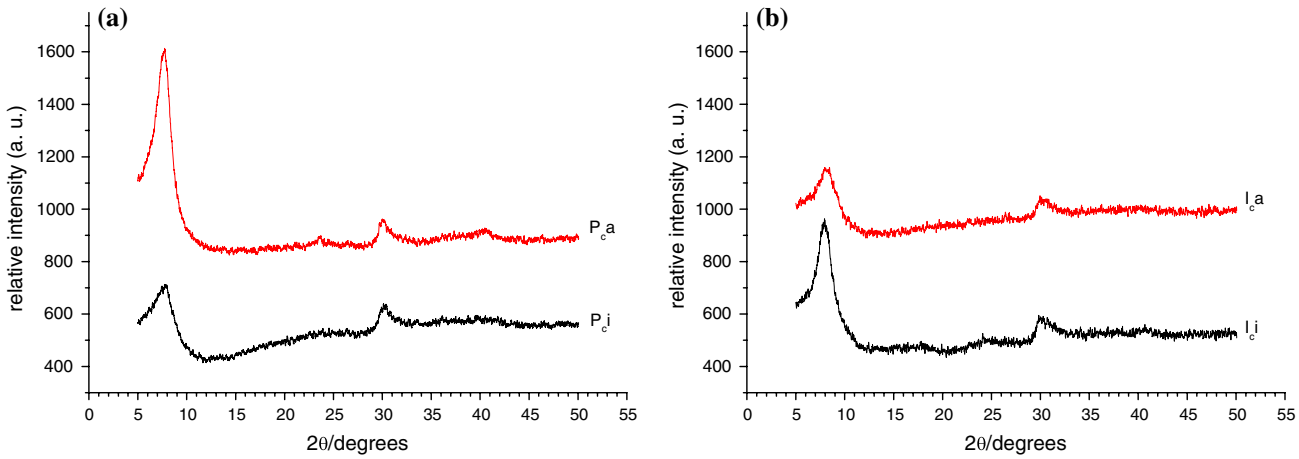


**Fig. 10** XRD patterns of as-prepared $V_2O_5$ powder samples prepared in: **a** $[Py_{1,4}]Tf_2N$ and **b** $[EMIM]Tf_2N$ with acetone and isopropanol (separately) as co-solvents. See Table 1 for abbreviations

produced particles [36]. Therefore, it seems of interest to employ the same procedure in synthesis of $V_2O_5$.

Vanadium pentoxide powders prepared in the two ionic liquids $[Py_{1,4}]Tf_2N$ and $[EMIM]Tf_2N$ using acetone and isopropanol as co-solvents show almost the same XRD patterns apart from sample $P_c$a ($[Py_{1,4}]Tf_2N$/acetone) which gives a product with higher crystallinity similar to that obtained in the case of using pure $[Py_{1,4}]Tf_2N$ ionic liquid and acetone as a refluxing solvent $P_r$a (Fig. 10). However, this method seems to rather affect the morphology of $V_2O_5$, since sample $P_c$i ($[Py_{1,4}]Tf_2N$/isopropanol) gives interestingly a ribbon-like morphology (Fig. 11). The other samples exhibit more or less the same rod-like morphology (not shown).

Thermal analysis (TGA and DTA) of the $P_c$a and $I_c$a samples, Fig. 12 shows quite similar behavior like the

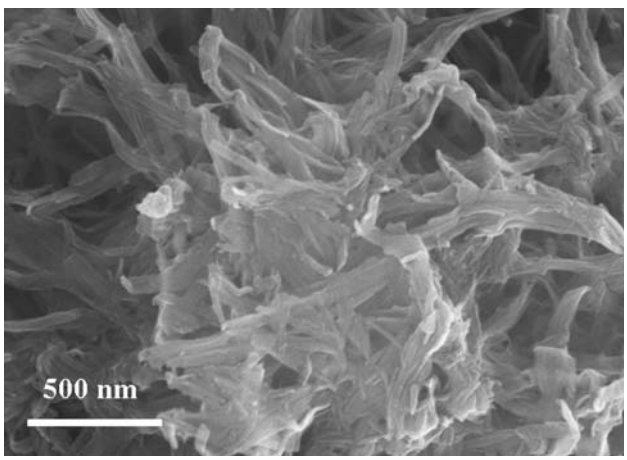


**Fig. 11** HR-SEM micrograph of $V_2O_5$ powder ($P_c$i)

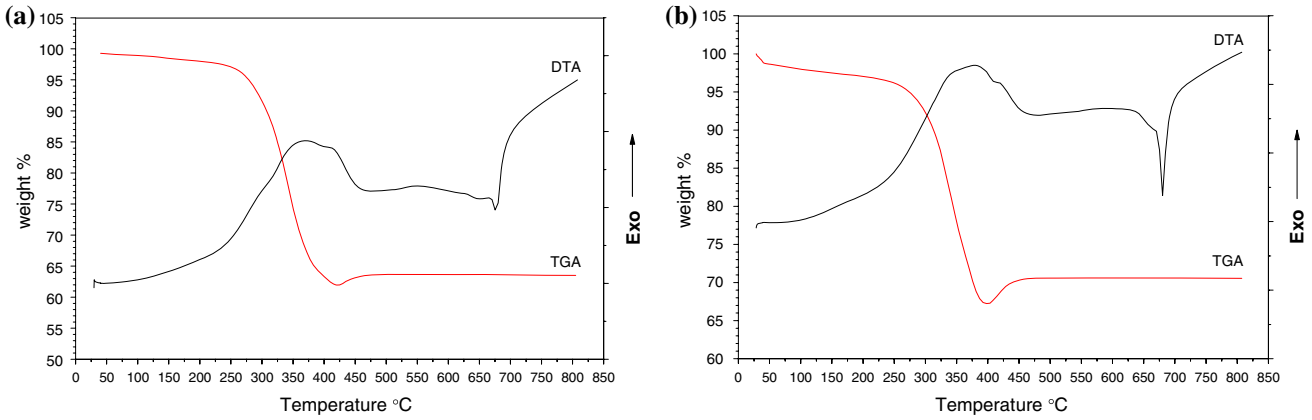


**Fig. 12** TGA and DTA curves of $V_2O_5 \cdot nH_2O$ powder samples: **a** $P_c$a and **b** $I_c$a

samples prepared in the pure ionic liquids with acetone as a refluxing solvent.

The surface area of the obtained samples was determined by BET measurements. $I_c$a (as-prepared sample) has the highest surface area of 36 $m^2$/g then $I_r$a sample of 23 $m^2$/g, while the $P_r$a and $P_c$a samples have very low surface areas of <3 $m^2$/g. This might be due to the difference in solubility of $[Py_{1,4}]Tf_2N$ and $[EMIM]Tf_2N$ in acetone or may be due to difference in interactions of cations $[Py_{1,4}]^+$ and $[EMIM]^+$ of the ionic liquid with negatively charged vanadium oxide layers surface. The negative oxygen (V=O) of the oxide layers can interact with organic cations placed between them [47].

## Conclusion

From the present work on the sol–gel synthesis of $V_2O_5$ in $[Py_{1,4}]Tf_2N$ and $[EMIM]Tf_2N$ ionic liquids, it can be concluded that the type of the cation of the ionic liquid as well as the organic solvent used either as a refluxing or as a co-solvent affect the crystallinity and morphology of the produced metal oxide: $V_2O_5$ with higher crystallinity and higher purity is obtained via hydrolysis in $[Py_{1,4}]Tf_2N$/acetone media as confirmed by XRD, DTA, and TGA measurements and mesoporous $V_2O_5$ can be synthesized in $[EMIM]Tf_2N$ ionic liquid especially when isopropanol is used either as a co-solvent or as a refluxing solvent.

The surface area of the produced metal oxide nanoparticles is strongly enlarged by acid hydrolysis of the metal alkoxide precursor: 88 $m^2$/g is the surface area of $V_2O_5$ obtained after acid hydrolysis of the employed precursor in $[EMIM]Tf_2N$. In contrast, the corresponding water hydrolysis in the same ionic liquid gave a surface area of 23 $m^2$/g.

Future studies on the effect of the anion type of the ionic liquid on the formation of $V_2O_5$ and insertion of lithium ions in this material for applications in lithium ion batteries are planned.

## References

1. Jolivet JP (2000) In: Metal oxide chemistry and synthesis, from solution to solid state. Wiley, England, pp 119–121
2. Livage J (1991) Chem Mater 3:578
3. Moshfegh AZ, Ignatiev A (1991) Thin Solid Film 198:251
4. Morin FJ (1959) Phys Rev Lett 3:34
5. Bystrom A, Wilhelmi KA, Brotzen O (1950) Acta Chem Scand 4:1119
6. Bachman HG, Ahmed FR, Barnes WH (1961) Z Kristallogr 115:110
7. Bahgat AA, Ibrahim FA, El-Desoky MM (2005) Thin Solid Film 489:68
8. Livage J (1984) Mater Res Soc Symp Proc 32:125
9. Barboux P, Baffier N, Morineau R, Livage J (1985) In: Goodenough JB, Jensen J, Potier A (eds) Solid state protonic conductors III. Odense University Press, Paris, pp 173–179
10. Spahr ME, Stoschitzki-Bitterli P, Nesper R, Haas O, Novák P (1999) J Electrochem Soc 146:2780
11. Zhang JG, McGraw JM, Turner J, Ginley D (1997) J Electrochem Soc 144:1630
12. Bazito FFC, Torresi RM (2006) J Braz Chem Soc 17:627
13. Gao L, Wang X, Fei L, Ji M, Zheng H, Zhang H, Shen T, Yang K (2005) J Crystal Growth 281:463
14. Shin DH, Bang CU, Hong YC, Uhm HS (2006) Mater Chem Phys 99:269
15. Lakshmi BB, Patrissi CJ, Martin CR (1997) Chem Mater 9:2544
16. Alonso B, Livage J (1999) J Solid State Chem 148:16
17. Hench LL, West JK (1990) Chem Rev 90:33
18. Reuter H (1991) Adv Mater 3:258
19. Brinker CJ, Scherer GW (1990) In: Sol–gel science: the physics and chemistry of sol–gel processing. Academic Press, New York, pp 31–43
20. Lin H, Kozuka H, Yoko T (1998) Thin Solid Film 315(1–2):111
21. Reuter H (1991) Adv Mater 3(11):568
22. Nabavi M, Doeuff S, Sanchez C, Livage J (1990) J Non-Cryst Solid 121(1–3):31
23. Seddon KR (1997) J Chem Technol Biotechnol 68:351
24. Earle MJ, Seddon KR (2000) Pure Appl Chem 72:1391
25. Ding KL, Miao ZJ, Liu ZM, Zhang ZF, Han BX, An GM, Miao SD, Xie Y (2007) J Am Chem Soc 129:6362
26. Adams CJ, Bradley AE, Seddon KR (2001) Aust J Chem 54:679
27. Zhou Y, Antonietti M (2004) Chem Mater 16:544
28. Zhou Y, Shattka JH, Antonietti M (2004) Nano Lett 4:477
29. Liu Y, Wang MJ, Li ZY, Liu HT, He P, Li JH (2005) Langmuir 21:1618

30. Huddleston JG, Willauer HD, Swatloski RP, Visser AE, Rogers RD (1998) Chem Commun 16:1765
31. Welton T (1999) Chem Rev 99:2071
32. Gordon CM, Holbrey JD, Kennedy AR, Seddon KR (1998) J Mater Chem 8:2627
33. Suarez PAZ, Selbach VM, Dullius JEL, Einloft S, Piatnicki CMS, Azambuja DS, de Souza RF, Dupont J (1997) Electrochim Acta 42:2533
34. Choi H, Kim YJ, Varma RS, Dionysiou DD (2006) Chem Mater 18:5377
35. Kaper H, Endres F, Djerdj I, Antonietti M, Smarsly BM, Maier J, Hu Y-S (2007) Small 3:1753
36. Al Zoubi M, Farag H, Endres F (2008) Aust J Chem 61:704
37. Yao T, Oka Y, Yamamoto N (1992) Mater Res Bull 27:669
38. Durupthy O, Steunou N, Coradin T, Maquet J, Bonhomme C, Livage J (2005) J Mater Chem 15:1090
39. Barbosa GN, Brunello CA, Graeff CFO, Oliveira HP (2004) J Solid State Chem 177:960
40. Wang X, Xie Y-C (2001) Catal Lett 75:73
41. Petkov V, Trikalitis PN, Bozin ES, Billinge SJL, Vogt T, Kanatzidis MG (2002) J Am Chem Soc 124:10157
42. Losurdo M, Barreca D, Bruno G, Tondello E (2001) Thin Solid Film 384:58
43. Olivetti EA, Kim JH, Sadoway DR, Asatekin A, Mayes AM (2006) Chem Mater 18:2828
44. Turova NY, Turevskaya EP, Kessler VG (2002) The chemistry of metal alkoxides. Kluwer Academic Publishers, Dordrecht
45. Livage J, Guzman G, Beteille F, Davidson P (1997) J Sol–Gel Sci Technol 8:857
46. Prandtl W, Hess L (1913) Z Anorgan Chem 82:103
47. Livage J (1998) Coordinat Chem Rev 178:999